Systematic Camera Placement Framework for Operation-Level Visual Monitoring on Construction Jobsites

Jinwoo Kim[1]; Youngjib Ham, Ph.D., A.M.ASCE[2]; Yohun Chung[3]; and Seokho Chi, Ph.D., M.ASCE[4]

Abstract: This paper proposes a camera placement framework that incorporates characteristics of complex construction jobsites. The proposed framework consists of three main processes: (1) identification of visual monitoring determinants, influencing factors, and camera placement conditions; (2) problem definition and mathematical modeling; and (3) hybrid simulation-optimization of camera placement on construction jobsites. To evaluate the performance of the proposed framework, a case study for an actual construction jobsite was performed. The results of the case study show the potential of the proposed framework to find the optimal number, types, locations, and orientations of cameras for jobsite visual monitoring. This research makes three main contributions: (1) identification of critical elements to be considered when installing fixed cameras on complex construction jobsites; (2) development of a systematic framework for camera placement on jobsites; and (3) visualization and quantification of multiple camera network designs and their performance (i.e., total costs and visible coverages) before installing cameras at actual jobsites. **DOI: 10.1061/(ASCE)CO.1943-7862.0001636.**

Author keywords: Visual monitoring; Operation-level; Construction jobsite; Camera placement; Optimization; Multiobjective; Art gallery problem; Genetic algorithm; Hybrid simulation-optimization.

Introduction

Today, a large amount of visual data is being collected for construction jobsite monitoring. Recent advances in unmanned aerial vehicles (UAVs) have helped practitioners regularly gather visual data (e.g., daily or weekly) and perform project-level monitoring with ease (e.g., progress measurement) (Teizer 2015). Many researchers have also investigated innovative UAV-based data collection/analysis methods for project-level visual monitoring (Ham et al. 2016). Despite the benefits of UAV-based data collection and monitoring, construction firms still need to install fixed cameras and capture long-sequence video streams for continuous operation-level monitoring on jobsites (Seo et al. 2015). Project-level monitoring primarily focuses on issues concerning the performance of output production (e.g., work amount of formwork) but does not capture in detail the performance of input resources (e.g., idle time of workers) (Yang et al. 2015). In contrast, continuous visual data collected by fixed cameras involves information on input resources, such as workers' activities. The continuous monitoring of such information enables measurements of operational efficiency (e.g., direct work rate, hourly work amount) and/or recognition of unsafe worker and equipment behavior (e.g., access to dangerous zones, speed limit violations). Thus, the operation-level information from camera networks can help project managers make better project-related decisions (e.g., resource allocations, scheduling) as well as evaluate on-site productivity and safety.

To effectively perform operation-level jobsite monitoring, camera placement—which determines number, types, locations, and orientations of fixed cameras required to sufficiently cover construction jobsites—is one of the most important but challenging issues. According to the authors' interviews with construction experts who had several experiences with installing digital cameras on jobsites, practitioners were observed to generally carry out camera placement based on their knowledge or experience rather than systematic guidelines. Their decisions occasionally come with acceptable visual monitoring performance (in term of camera coverage or total costs) but often encounter difficulties with determining proper camera configurations because of a number of unique conditions to be considered in given complex jobsites: for example, power supply, data transmissibility, and occlusion effects. Those conditions make the manual camera placement process time consuming and labor intensive and may cause performance deviations in jobsite visual monitoring. For instance, the actual coverage of installed cameras differs from project managers' expectations; as such, target monitoring regions (e.g., work zones, travel path) are often invisible from the installed cameras. In this regard, a question could arise as to whether certain camera placement and coverage are the best for visual monitoring of given jobsites. Many researchers in academia have extensively studied the art gallery problem (AGP)—a well-documented open research challenge to find the optimum sensor network design under given constraints—to optimize

[1]Ph.D. Candidate, Dept. of Civil and Environmental Engineering, Seoul National Univ., 1 Gwanak-Ro, Gwanak-Gu, Seoul 08826, Republic of Korea; Researcher, Institute of Construction and Environmental Engineering, Seoul National Univ., 1 Gwanak-Ro, Gwanak-Gu, Seoul 08826, Republic of Korea. Email: jinwoo92@snu.ac.kr

[2]Assistant Professor, Dept. of Construction Science, Texas A&M Univ., 3137 TAMU, College Station, TX 77843. Email: yham@tamu.edu

[3]Assistant Manager, Investment Division 1, IGIS Asset Management, 115 Yeouigongwon-Ro, Yeongdeungpo-Gu, Seoul 07241, Republic of Korea. Email: yohun.chung@igisam.com

[4]Associate Professor, Dept. of Civil and Environmental Engineering, Seoul National Univ., 1 Gwanak-Ro, Gwanak-Gu, Seoul 08826, Republic of Korea; Adjunct Professor, Institute of Construction and Environmental Engineering, Seoul National Univ., 1 Gwanak-Ro, Gwanak-Gu, Seoul 08826, Republic of Korea (corresponding author). Email: shchi@snu.ac.kr

Note. This manuscript was submitted on May 23, 2018; approved on September 28, 2018; published online on February 15, 2019. Discussion period open until July 15, 2019; separate discussions must be submitted for individual papers. This paper is part of the ***Journal of Construction Engineering and Management***, © ASCE, ISSN 0733-9364.

camera placement in buildings and urban areas (Altahir et al. 2017; Hörster and Lienhart 2006; Nguyen and Bhanu 2011; Zhao et al. 2013).

Although these previous studies provide an encouraging proof-of-concept that supports camera placement decisions, they have primarily focused on camera placement in relatively organized environments (e.g., building/urban areas with power accessibility) for security/traffic monitoring. Thus, determining optimal camera configurations considering various unique conditions of complex construction jobsites (e.g., power accessibility, facilities, and work zones) is still challenging. To address such a challenge, this paper proposes a new, systematic camera placement framework that incorporates the characteristics of construction jobsites. The objective of the framework is to determine the set of types, number, locations, and orientations of fixed cameras that maximizes meaningful camera coverage and minimizes the total costs for installing camera networks under given jobsite constraints. This research makes three main contributions: (1) identification of critical elements to be considered when installing fixed cameras on complex construction jobsites; (2) development of a systematic framework for camera placement on jobsites; and (3) visualization and quantification of multiple camera network designs and their performance (i.e., total costs and visible coverages) before installing cameras on actual jobsites.

This paper is organized as follows. After the introduction, this paper reviews previous works on operation-level visual monitoring in construction jobsites and the AGP for camera placement. Next, details of the proposed framework for optimizing camera placement at construction jobsites are explained. To validate the proposed framework, the case study and results analyses are then performed. Finally, this paper discusses contributions and future works in the conclusions.

Literature Review

Operation-Level Visual Monitoring on Construction Jobsites

Operation-level visual monitoring is commonly conducted to better understand on-site productivity and safety. Given the importance, practitioners have installed multiple fixed cameras and have performed manual observation to extract operation-level information (e.g., work durations of workers allocated to a certain type of activity). However, the human-based manual monitoring requires extra time and costs to process a large amount of video/image data (Kim and Chi 2017). To overcome such limitations, automated vision-based monitoring systems and remote monitoring technologies have been introduced to facilitate productivity and safety analysis. Many studies have presented vision-based equipment activity recognition methods for equipment operation and productivity analysis. Golparvar-Fard et al. (2013), for instance, proposed a framework that recognizes the actions of single earthmoving equipment from a site's video stream. The proposed method by Kim et al. (2018d) identified activity types considering interactions between excavators and dump trucks. Based on the identified activities, the dirt-loading cycle time of an excavator and a dump truck was analyzed by Rezazadeh Azar et al. (2013). Bügler et al. (2017) also presented a method that automatically measures the productivity of earthmoving operations through photogrammetry and video analysis. In Kim et al. (2018a), such operational information obtained from visual analytics (e.g., direct work rate and cycle time) has been further integrated into construction process simulation models to estimate earthmoving productivity and project-completion time.

Researchers have also developed construction worker activity recognition methods to automate work sampling and productivity assessments. The methods proposed by Luo et al. (2018b, d), for example, classified activity types by capturing the spatial and temporal information of a single worker. Luo et al. (2018c) furthermore presented a method that recognizes construction activities by detecting multiple construction resources (e.g., workers, equipment, and materials) and analyzing their spatial relations (e.g., size and distance).

Regarding safety management, Chi and Caldas (2012) proposed an image-based safety assessment method for surface mining activities. The method tracked the locations of earthmoving equipment and assessed spatial risks based on their movements (e.g., speed and proximity) and safety rules (e.g., speed limits). In addition to the risk assessment, Kim et al. (2016) applied fuzzy inferences to support the rapid risk awareness of construction workers who are the major victims of accidents. The vision-based analysis was also adapted to detect human's unsafe behaviors. Han and Lee (2013) identified a list of critical body postures and motions from accident statistics and checklists that cause ergonomic injuries. They developed a method that recognizes workers' unsafe postures and motions from stereo images. The method in Ding et al. (2017) also detected unsafe worker behavior by using convolutional neural networks and long short-term memory. Because wearing personal protection equipment (PPE) is a major indicator of the understanding of workers' unsafe behavior, Park et al. (2015) and Fang et al. (2018b) presented an automated monitoring method that detects non-hardhat-wearing workers from surveillance cameras. Fang et al. (2018a) and Fang et al. (2018c) extended prior works for monitoring various PPE-wearing states, such as safety harnesses and anchorages.

The aforementioned research focuses on a visual data analysis toward semiautomation or automation of operation-level visual monitoring. However, most studies are based on an underlying assumption: video/image data collected from actual construction jobsites have acceptable and reliable quality for realizing the benefits of computer vision techniques (Seo et al. 2015; Yang et al. 2015). This assumption infers that the developed vision-based systems would be prone to errors if occlusions or an unclear camera field-of-view (FOV) occur. Given such an issue, many researchers have claimed that visual data collection—camera placement—should be studied to enhance both the performance of visual analytics and the practicality of automated jobsite visual monitoring (Kim et al. 2018d; Rezazadeh Azar et al. 2013; Seo et al. 2015). The proper camera placement can also benefit manual visual monitoring by capturing useful data while reducing unnecessary data (e.g., heavily occluded view).

Art Gallery Problems for Camera Placement and Current Practices in Construction

The AGP originated from the challenges in determining the minimal number of guards and their locations required to cover the interior of an art gallery (Hörster and Lienhart 2006). Because general camera placement problems are similar to the AGP (Ahn et al. 2016; Hörster and Lienhart 2006), AGP theorems and algorithms have been studied to find the optimal camera placement in various domains.

In the camera surveillance domain, researchers first focused on maximizing fixed cameras' coverage to monitor target objects (e.g., human, vehicle) and unexpected events (e.g., crime, traffic accident) in indoor and built environments (Hörster and Lienhart 2006; Morsly et al. 2009; Murray et al. 2007). Omnidirectional and pan-tilt-zoom (PTZ) cameras were also considered for

coverage modeling and maximization problems (Altahir et al. 2017; Gonzalez-Barbosa et al. 2009; Indu et al. 2009). Recently, the camera placement problems have been extended to multiobjective optimization that not only maximizes cameras' coverage but also minimizes investment costs (Ahn et al. 2016; Altahir et al. 2017; Zhao et al. 2013). To solve the defined problems with a reasonable practical range of accuracy, researchers have also tested the applicability of metaheuristic optimization algorithms for camera placement (Abdesselam and Baarir 2018; Aissaoui et al. 2017; Al-Hmouz and Challa 2005). Building on previous research, camera placement optimization techniques were further leveraged for a series of domain-specific applications. For example, the camera placement problem was reformulated to optimize the performance of visual analytics (e.g., reconstruction and motion captures) (Olague and Mohr 2002; Rahimian and Kearney 2017) and automated surveillance systems in urban areas (Bodor et al. 2007; Szaloki et al. 2013). In the construction domain, as the first step to addressing the AGP for optimal camera placement, the camera's coverage was computationally modeled to understand and evaluate the visibility of installed cameras. Chen et al. (2013) developed a visualization technique to measure the coverage of camera networks in public building spaces. Based on coverage visualization and simulation, project stakeholders would communicate better and make proper decisions—camera placement planning. Albahri and Hammad (2017a) proposed a method to calculate coverage of cameras installed in buildings using building information modeling (BIM). The BIM-based coverage calculation method was then applied to the camera optimization problems in Albahri and Hammad (2017b). The research optimized camera placement in indoor spaces using BIM-based camera coverage and cost calculations. In the optimization process, BIM played a key role in automatically deriving installation conditions, such as geometrical constraints (e.g., ceiling) and operational constraints (e.g., vibration produced by facility components).

Previous research showed promising results in optimizing camera placement to monitor indoor spaces and urban areas. Despite such efforts, the authors' extensive survey/interview implies that construction practitioners still place cameras based on their knowledge or experiences rather than systematic guidelines primarily because the existing camera placement methods are likely limited to security/traffic monitoring purposes in relatively organized environments (e.g., building/urban areas with power accessibility). However, visual monitoring on outdoor construction jobsites have unique characteristics with different operation-level monitoring purposes and case-oriented camera placement conditions (e.g., power accessibility, facilities, and work zones). Thus, generalizing the optimal configurations of fixed cameras to be installed on complex construction jobsites with minimized costs is still challenging; for instance, the actual coverage and/or total costs of installed cameras are likely different from project managers' expectations. To fill such a knowledge gap, this paper proposes a new systematic camera placement framework that incorporates the characteristics of complex construction jobsites for visual monitoring.

Research Framework

The research framework consists of three main parts. First, the authors identify critical visual monitoring determinants, influencing factors, and camera placement conditions for installing fixed cameras on construction jobsites via expert interviews. Next, based on the interview results, problem definition and mathematical modeling are performed to reflect the unique characteristics of the given construction jobsites. Finally, the hybrid simulation-optimization processes are carried out to solve the defined problems. The details of each procedure are given in the following sections.

Identification of Visual Monitoring Determinants, Influencing Factors, and Camera Placement Conditions

To understand and identify practical characteristics of construction jobsites, the authors conducted face-to-face and semi-structured interviews. In particular, the research team performed expert interviews one-by-one until information saturation was observed in the same manner as in previous interview-driven studies, including Biggs et al. (2013) and Zhang et al. (2017). For interviewee selection, convenience sampling and snowball sampling methods were used (Auerbach and Silverstein 2003). As a result, a total of 12 experts were interviewed in accordance with their organization types (i.e., construction firms, camera installation firms, and research institutes), positions and duties, and professional experiences. Among the 12 interviewees, eight experts had experience installing cameras at construction jobsites. In the case of construction experts, most interviewees were engaged in different project types (i.e., road construction, new-town development, factory construction, office building, and residential building), which enabled avoidance of sampling bias and reflected various jobsite characteristics. Three of the interviewees had experience with constructing camera networks for jobsite monitoring purposes. Three project managers and three assistant managers had worked in the construction industry for more than twenty and five years, respectively. In addition, four camera network designers and installation engineers were interviewed to identify camera-related issues at jobsites. Because they had designed and installed cameras for at least 10 years and all had experience installing cameras on construction jobsites, deriving important issues related to camera placement was expected. Lastly, the research team interviewed two visual data analysts. Although both interviewees had more than five years of experience, they were from different domains: construction jobsite monitoring and computer vision. The jobsite monitoring expert had experience with developing camera networks at actual construction jobsites.

The interview results are summarized in Table 1. Four major visual monitoring determinants existed: visual monitoring purposes, visible coverage, total costs, and installable locations. Each determinant could be explained using several influencing factors, and each influencing factor was then subdivided into specific placement conditions of the camera network and the jobsite. First, all interviewees mentioned that the monitoring purpose should be clearly defined by construction managers when planning camera placement at jobsites. According to six construction experts, visual monitoring purposes could be decomposed into two main influencing factors: construction operations and on-site logistics. They pointed out construction operations as the primary monitoring purpose; therefore, jobsite camera networks are expected to cover work zones because long-sequence videos recorded from work zones can provide project managers with operation-level information on workers and equipment (e.g., hourly productivity). The on-site logistics (i.e., material-flows) also raised the attention of three experts given their significant impact on activity planning and coordination. They suggested two main coverage areas for monitoring on-site logistics: travel paths and storage yards. Interpreting videos from the two areas can identify locations and quantities of materials transported by workers or equipment (e.g., concrete and mixer trucks). Second, visible coverage of installed cameras was selected as a key determinant in the evaluation of the performance of camera networks for jobsite visual monitoring. In particular, camera

Table 1. List of visual monitoring determinants, influencing factors, and camera placement conditions on construction jobsites

Visual monitoring determinant	Influencing factor	Description	Camera placement condition	
			Camera network condition	Jobsite condition
Monitoring purposes	Construction operations	Understanding operational performance of workers and equipment	—	Work zones
	On-site logistics	Identifying material-flows for activity planning and coordination	—	Travel paths Storage yards
Visible coverage	Total coverage without occlusions	Total coverage of installed cameras without occlusion effects	Number of cameras Camera types	—
	Occlusions	Major cause in decreasing visible coverage and interrupting visual monitoring tasks	Camera locations Camera orientations	Facilities Long-term-standing equipment
Total costs	Installation costs	Costs for installing cameras at certain locations	Number of cameras Camera locations	Facilities —
	Purchasing costs	Cost for purchasing cameras	Camera types Number of cameras	—
Installable locations	Workflow disturbance	Physical intervention in construction operations and on-site logistics	Camera locations	Semi-permanent facilities Permanent facilities Work zone Travel path Storage yards Temporary facilities Work zones
	Power accessibility	Availability to activate activating cameras continuously	Camera locations	Locations of power suppliers
	Data transmissibility	Availability to transfer and save visual data in storage	Camera locations	Transmitter locations

network designers and visual data analysts clarified that visible coverage is determined by two influencing factors: total coverage with and without occlusions. Total coverage without occlusions can be further subdivided into types and number of cameras to be installed. In the meantime, all of the interviewees had the consistent opinion that occlusions should be kindly considered. The two visual data analysts and three construction managers highlighted the effects of static occlusions caused by facilities or long-term-standing equipment because static occlusions could continually not only decrease visual data quality but also have negative impacts on visual monitoring (e.g., the case in which construction operations are invisible from cameras in the long term). Participants also mentioned that considering the negative effects of dynamic occlusions caused by moving workers and equipment is needed; however, they further pointed out that dynamic occlusions would be robustly addressed by postprocessing given their relatively short durations. This finding encouraged the authors to primarily focus on minimizing the negative effects of static occlusions. In this context, locations and camera orientations should be well-decided considering the causes of major occlusions at jobsites, such as facilities (e.g., management offices) and long-term-standing equipment (e.g., tower crane).

Third, the total cost for jobsite camera networks was mainly discussed by industry experts. Obviously, all construction experts had expectations of installing cameras with minimal total costs that are less than their limited budgets. Total costs are composed of cameras' installation and purchasing costs. The camera installation engineers stated that installation fees are derived using two camera network conditions: number of installations (i.e., cameras) and camera locations. The installation fees can increase when additional apparatus (e.g., brackets, supports, power generators) or labor input are required. In contrast, installation fees can be avoided or reduced if possible through easy installation of cameras at facilities without extra apparatus. Lastly, construction and camera experts regarded installable locations of cameras as an important visual monitoring determinant. All of the construction experts asserted that installed cameras should not disturb construction workflows, such as activities of workers and equipment in work zones, movements in travel paths, and material loading in storage yards. In this regard, they further suggested boundaries for semi-permanent or permanent facilities (e.g., fences, long-term standing equipment, management offices) as installable locations. They also assigned work zones, travel paths, storage yards, and temporary facilities (e.g., temporary supports to be transported or assembled shortly) to noninstallable locations. Technical factors such as power accessibility and data transmissibility were also considered by camera installation firms. The two influencing factors can be explained with locations of cameras, power suppliers, and transmitters.

Through extensive interviews, the authors were able to understand important visual monitoring determinants, influencing factors, and camera placement conditions on construction jobsites, as summarized in Table 1. Based on the findings, the next section describes the research team's efforts in defining the problem and carrying out mathematical modeling for camera placement optimization.

Problem Definition and Mathematical Modeling

The goal of this paper is to determine the optimal number, types, locations, and orientations of fixed cameras that maximize visible coverage and minimize total costs of a camera network given

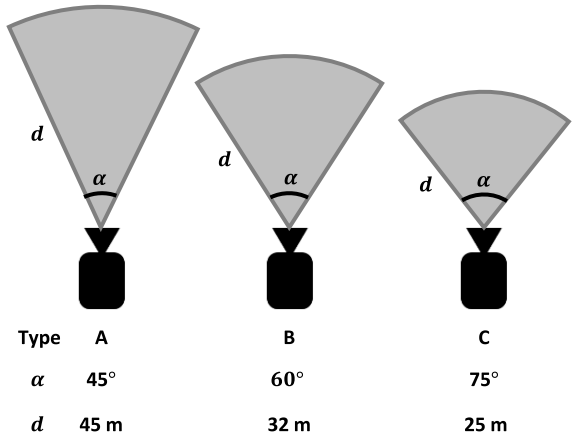

Fig. 1. Examples of camera coverage modeling.

jobsite-specific constraints (e.g., limited budgets, installable locations). In this sense, a need exists to formulate and address a multiobjective optimization problem to maximize visible coverage and minimize total costs under given jobsite constraints. The coverage of fixed cameras without occlusions can be modeled depending on their visible distance and angle of view (i.e., camera types), as illustrated in Fig. 1. For the spatial modeling of given jobsites, three-dimensional aspects (i.e., width, length, and height) of jobsite components (e.g., facilities, structures) are represented in grid maps with n rows and m columns, along with height information. The size of each grid was set as 1×1 m, considering the surveillance cameras' dimension with a space buffer (AXIS Communication 2017) and based on the experts' suggestions.

To address the defined problem, the mathematical modeling was performed as follows. There are two objective functions [Eqs. (1) and (2)]. Eq. (1), the first objective function, aims to maximize the total weighted visible coverage of all cameras. By involving the spatial-contextual importance of each cell $w_{i_2 j_2}$, it enables finding camera configurations that cover target monitoring areas (e.g., work zones, travel paths) with a limited number of cameras. The idea is that project managers can discriminatively focus on target areas (e.g., dangerous zones) with higher weights and then gather visual data for specific monitoring purposes (e.g., safety monitoring). The second objective function [Eq. (2)] is formulated to minimize the total costs of a camera network, which include purchasing and installation costs. The formulated multiobjective problem is constrained with Eqs. (3)–(7). The first constraint [Eq. (3)] indicates that the total costs should be less than the limited budgets. The purchasing costs can be calculated by multiplying the unit price by the number of cameras. Installation costs are accumulated with cost c_{ij} if a camera is located at a cell (i, j). Camera installation engineers assign installation costs for each cell depending on the need for additional apparatus or labor input. The second constraint [Eq. (4)] indicates that the total weighted coverages of installed cameras should be larger than certain weighted coverages; this constraint secures the minimum monitoring performance. Eq. (5) indicates that all cameras should be located at installable locations. Installable locations are determined by three jobsite conditions: facility boundaries b_{ij}, power accessibility p_{ij}, and data transmissibility d_{ij}. If at least one jobsite condition is not met (i.e., if one of the three variables is zero), camera installation is not available. To ensure that only one camera is located at each cell, including Eq. (6) is necessary. Lower/upper bound constraints on locations and orientations are expressed in Eq. (7).

Objective function 1: to Maximize the Total Weighted Visible Coverages of Cameras

$$\max \sum_{\theta} \sum_{i} \sum_{j} x_{i_1 j_1 \theta_1} * e_{i_1 j_1 \theta_1 i_2 j_2} * w_{i_2 j_2} \tag{1}$$

Objective function 2: to minimize the total costs of the camera network

$$\min UP * \sum_{\theta} \sum_{i} \sum_{j} x_{ij\theta} + \sum_{\theta} \sum_{i} \sum_{j} x_{ij\theta} * c_{ij} \tag{2}$$

Subject to

$$UP * \sum_{\theta} \sum_{i} \sum_{j} x_{ij\theta} + \sum_{\theta} \sum_{i} \sum_{j} x_{ij\theta} * c_{ij} \le Budgets \tag{3}$$

$$\sum_{\theta} \sum_{i} \sum_{j} x_{i_1 j_1 \theta_1} * e_{i_1 j_1 \theta_1 i_2 j_2} * w_{i_2 j_2} \ge CR * \sum_{i} \sum_{j} w_{\mathrm{ij}} \tag{4}$$

$$\sum_{\theta} x_{ij\theta} \le b_{ij} * p_{ij} * d_{ij} \quad for\ \forall i, j \tag{5}$$

$$\sum_{\theta} x_{ij\theta} \le 1 \quad for\ \forall i, j \tag{6}$$

$$1 \le i \le n, 1 \le j \le m, 0 \le \theta \le 360 \tag{7}$$

where the binary variable $x_{ij\theta}$ represents whether a camera is located at a cell (i, j) with orientation θ; $e_{i_1 j_1 \theta_1 i_2 j_2}$ indicates whether a cell (i_2, j_2) is covered by a camera that has an orientation θ and is located at (i_1, j_1); w_{ij} indicates the spatial-contextual weight of a cell (i, j); UP is a constant variable for the unit price of each camera; c_{ij} is a cost variable that represents the cost required to install a camera at cell (i, j); and CR is a fixed variable for the minimum coverage ratio of a camera network. The binary variables for installable locations, b_{ij}, p_{ij}, and d_{ij}, denote whether a cell (i, j) is included within facility boundaries and effective areas of power accessibility and data transmissibility.

In the defined problem and mathematical modeling, as a proof-of-concept in this paper, a camera type is fixed (i.e., a camera network is composed of a single type of cameras) given the following practical issues. According to the expert interviews, construction practitioners prefer to be provided with several network design alternatives for each camera type rather than only one optimal solution with a mixture of camera types. The experts from camera installation firms also noted that installing a sole type of camera with the same visible distance and angle of view for monitoring purposes is more common. However, worth mentioning is that various camera types can be optimized; therefore, project managers can compare multiple network design alternatives for each camera type. The next section explains a hybrid simulation-optimization procedure of the defined problem and mathematical modeling.

Hybrid Simulation-Optimization of Camera Placement on Construction Jobsites

The camera placement problem is known to be a nondeterministic polynomial time hard (NP-hard problem) (Cole and Sharir 1989; O'Rourke 1987) that has high dimensionality of the search space and nonlinearity among decision variables, objective functions, and constraints (Aissaoui et al. 2017). This statement infers that simple iterative search algorithms will most likely have difficulty finding the optimal solution. For these reasons, researchers have attempted to study a number of metaheuristic optimization

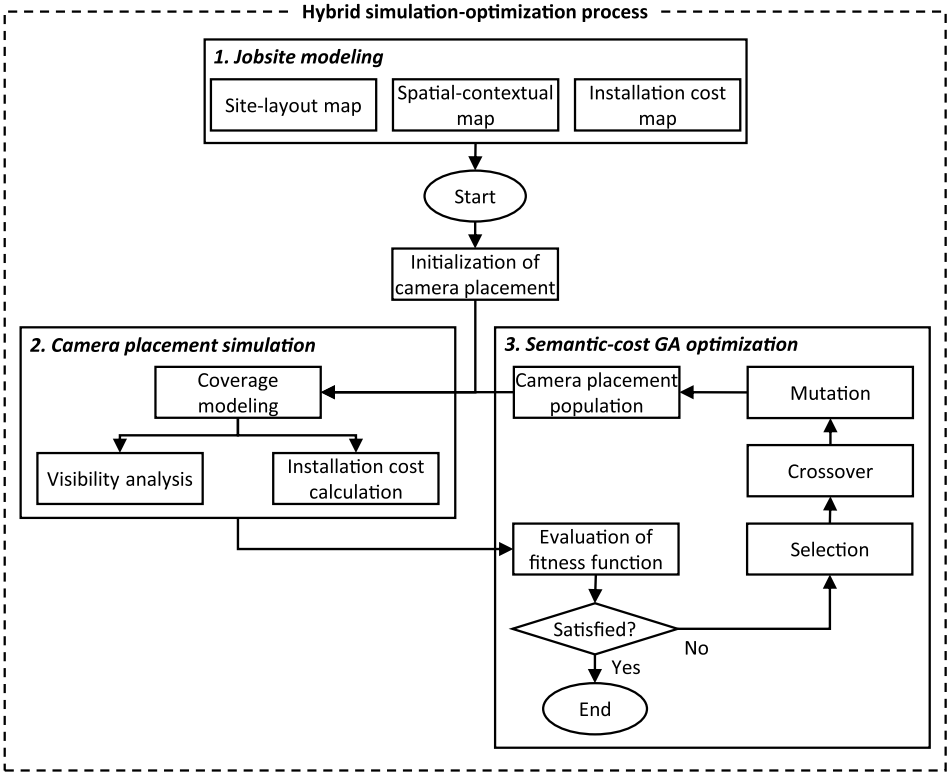

Fig. 2. Overview of proposed method.

algorithms to address camera placement problems. Among those metaheuristic algorithms, this research builds on the genetic algorithm (GA) to address the problems defined by the following benefits. The GA can find near global optimum trade-offs between multiobjectives because it tends not to get stuck at a local optimum (Bandyopadhyay and Pal 2007). This nature further enables effective management of the high dimensionality and nonlinearity of NP-hard problems. Additionally, the applicability of the GA has been extensively validated to address NP-hard problems, including camera placement optimization (Abo-Zahhad et al. 2014).

In particular, the authors integrated camera placement simulation into GA optimization in order to evaluate the objective functions with suggested camera configurations; in this paper, this integration is called a hybrid simulation-optimization process. Fig. 2 shows a hybrid simulation-optimization process composed of jobsite modeling, camera placement simulation, and semantic-cost GA optimization. Jobsite modeling is performed to encode jobsite-specific conditions (e.g., work zones, travel paths, and facilities) to computer-understandable representations. A total of three different jobsite maps are generated: site-layout, spatial-contextual weight, and installation cost. Once all of the encoded data (i.e., jobsite maps) are derived, camera configurations (i.e., number, locations, and orientations of cameras) are randomly initialized based on installable locations of the given site-layout map (i.e., boundaries of facilities); however, project managers can also initialize a set of potential camera configurations as they want. Such initial information is fed into the camera placement simulation, and then the performance of camera network designs is quantitatively evaluated through coverage modeling, visibility analysis, and installation cost calculations. Based on the simulation results, fitness functions are evaluated for whether or not it satisfies the terminal conditions. If satisfied, the optimization procedure is ended. If not, the semantic-cost GA optimization, reproduction of camera configurations, and camera placement simulation processes are iteratively conducted. More details on each process are given in the following subsections.

Jobsite Modeling

Fig. 3 illustrates examples of jobsite modeling for the site-layout, spatial-contextual weight, and installation cost maps. First, the site-layout map is derived from actual site-layouts (e.g., drawings or top-view images) that involve locations and dimensions of jobsite components (e.g., facilities, work zones). Here, different numeric values are assigned to each element or region (e.g., facilities, work zones, travel paths, and storage yards). For that purpose, cell-based user-friendly software such as Microsoft Excel can be used. Once the site-layout map is created, occlusion causes (e.g., facilities), installable locations (e.g., boundaries of facilities), and target monitoring areas (e.g., work zones and travel paths) are automatically identified using image processing algorithms such as edge detection. In addition, to consider the height of the camera placement in some cases, the proposed method assigns numeric values that indicate the height of each location in cells of occlusion causes and camera-installable locations; the occlusion cells are then activated when their height values are larger than the value of camera-installable locations and vice versa. Next, the weight map represents the spatial-contextual importance of each cell and is used to calculate the first objective function: the total weighted visible coverages. The spatial-contextual weights are allocated through user-guided probability distributions. When users designate certain points of interest (e.g., work zones, travel paths) depending on their monitoring purposes (e.g., operation/on-site logistic management), the weights of the surrounding points are determined based on a bivariate probability distribution (distance from the points of interests). This user-guided probability distribution enables representation of the continuous nature of workspaces and operational contexts on construction jobsites. This distribution indicates that

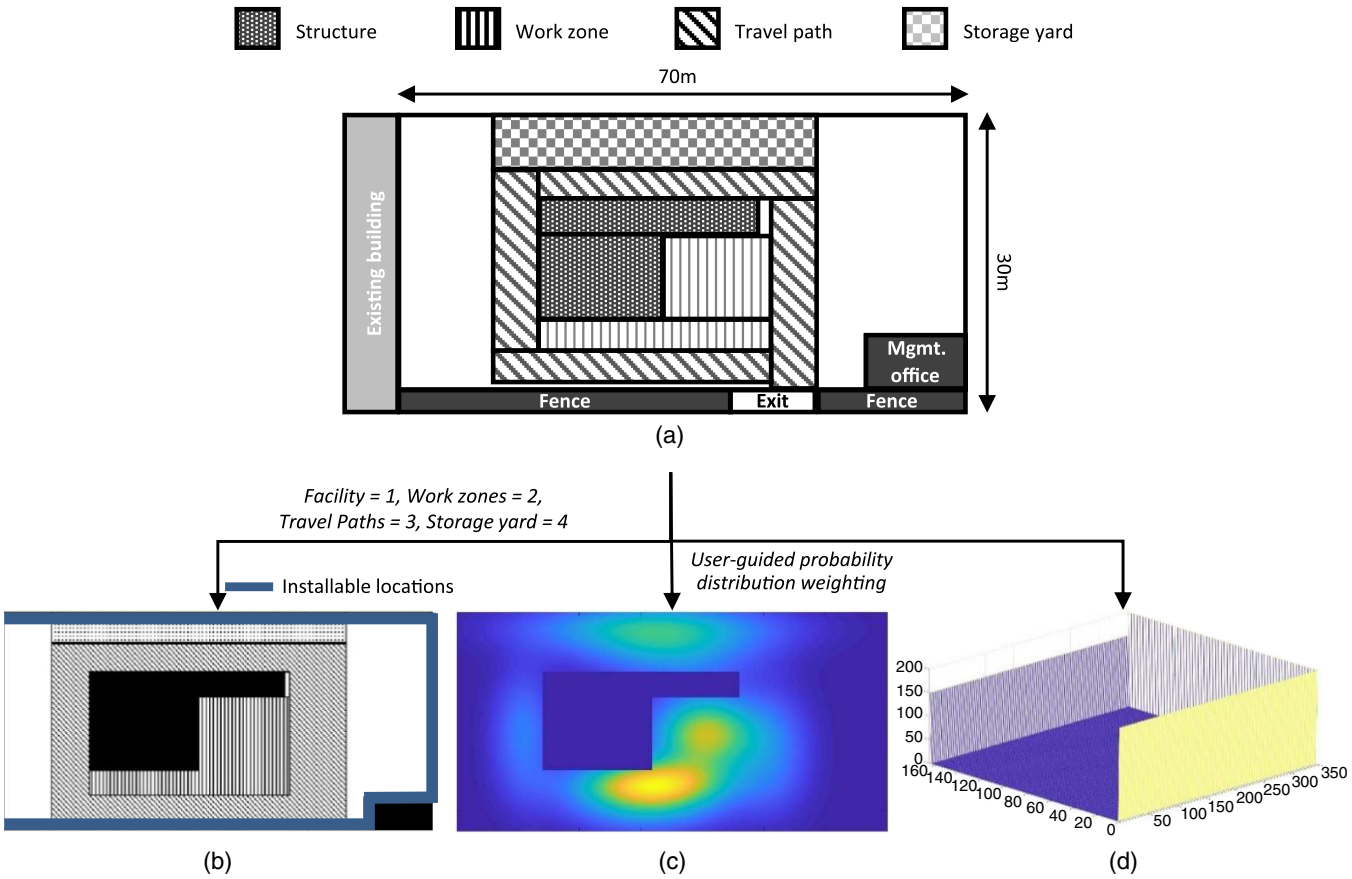

Fig. 3. Examples of jobsite modeling: (a) actual site-layout; (b) site-layout map; (c) spatial-contextual weight map; and (d) installation cost map.

the spatial-contextual importance of jobsite areas would decrease gradually as the distance from the points of interests increases; for example, the number of construction resources that are operation-level monitoring targets and that may exist or operate increases as the distance to the center of work zones decreases. The weighting method also allows camera networks to specialize in project managers' monitoring purposes by allocating greater importance values to target areas. Lastly, the installation cost map literally denotes the costs to install a camera at each cell. Whether or not additional apparatus and labor input are needed is determined.

Following jobsite modeling, the initialization of camera placement proceeds based on the installable locations on the site-layout map. Uniform distribution-based random sampling is used to produce initial number, locations, and orientations of cameras such that they satisfy the given constraints (e.g., less than budgets). Randomly generating a set of camera configurations is expected to decrease the possibilities to generate biased initial conditions and to be stuck at a local optimum.

Camera Placement Simulation

Camera placement simulation plays a major role in quantifying the performance of given camera configurations. The simulation process includes coverage modeling, visibility analysis, and installation cost calculations (Fig. 2). Coverage modeling computes camera coverages without occlusions based on the visible distance and angle of view of each camera type. This study is built on a sectorial representation for the camera coverage shown in Fig. 1. Next, visibility analysis is performed to examine occlusion effects (Fig. 4). Visibility is noted as relying on the line-of-sight from the camera viewpoint to the coverage points (i.e., cells within the camera coverage). Because all points in the same line-of-sight should have an equal rotation angle (α or β) with respect to the center point of the camera location, the line-of-sights can be extracted after computing rotation angles of all coverage cells. In the extracted line-of-sight, whether or not occlusion causes are included is confirmed. If included, the cells behind the occlusion causes (i.e., cells farther than the occlusion points from cameras) are determined to be "invisible" points. For the opposite case, all cells in the batch are allocated as "visible" coverage. During this process, occlusion causes are primarily activated through a comparison with the height values of the camera locations. All processes are repeated for every line-of-sight and camera. At the end, the simulation obtains the visible coverage of a given camera placement. Installation costs can be calculated using the locations of cameras and the installation cost map. Eventually, the results are fed into the semantic-cost GA optimization to evaluate the fitness function and produce better camera network designs.

Semantic-Cost GA Optimization

The semantic-cost GA optimization procedure is used to determine better camera network designs by evaluating the performance of prior conditions based on jobsite semantic coverage (i.e., visible coverage calculated using the spatial-contextual weight map) and total costs, and by iteratively performing population evolutions. In this paper, a chromosome indicates the configurations of a camera network (i.e., single alternative for camera network design) and population indicates a group of individual chromosomes of a certain generation (i.e., a set of camera network designs). The performance evaluation calculates the fitness values of each chromosome based on the results of the camera placement simulation. The total weighted visible coverages are computed using the

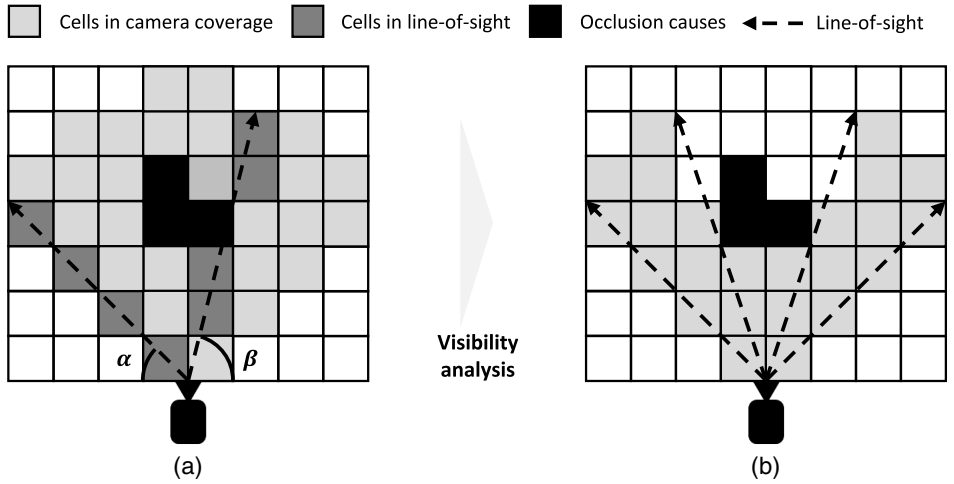

Fig. 4. Concept of visibility analysis and camera placement simulation: (a) before visibility analysis; and (b) after visibility analysis.

spatial-contextual weight map and the obtained visible cells [Eq. (1)]. The total costs can also be calculated using the purchasing and installation costs given from the camera placement simulation [Eq. (2)]. After the performance evaluation, the following two terminal conditions, which are derived in the heuristics experiments, are confirmed. When the best fitness values are constant for 50 generations, the interpretation is that the GA finally found the global optimum; then, the entire optimization procedure is halted. The other terminal condition is whether the total generations are greater than 100. For all iterations for which the terminal conditions are not met, the population evolution proceeds as follows.

The population evolution is carried out using the selection, crossover, and mutation (Fig. 5). The selection step chooses a subset of chromosomes with higher fitness values from the prior population (i.e., a set of chromosomes at the previous iteration). This research builds on the stochastic uniform selection method that allocates probability values for each chromosome proportional to its performance (fitness values), and then stochastically selects a part of the population based on the assigned selective probability. This selection method enables not only inheritance of elite chromosomes at a certain generation (i.e., elite protection) but also maintenance of the possibility of escaping out from a local optimum. Next, 5% of the selected chromosomes remain to secure the best solutions for each population, and the other 95% proceeds to the crossover and mutation. Among the 95%, 80% and 20% of the chromosomes were further split into crossover and mutation, respectively; the mutation process additionally proceeds for the noninherited chromosomes in the selection step to maintain the fixed population size. The crossover algorithm in this paper is partially based on the scattered method in Spall (2003). In particular, this study customized the method to prevent nonmeaningful crossover between irrelevant attributes; for instance, numeric location values are not transitioned to orientation and vice versa. For the mutation, the authors integrated the adaptive feasible method (Foster 2000) with the uniform distribution-based random sampling because the method from Foster (2000) can promote the last successful mutation (i.e., step length and direction) and random sampling can discover potential elite chromosomes. The population evolution processes are repeated until the aforementioned terminal conditions are satisfied.

For a detailed explanation of the semantic-cost GA processes, the following example is given, as indicated in Fig. 5.

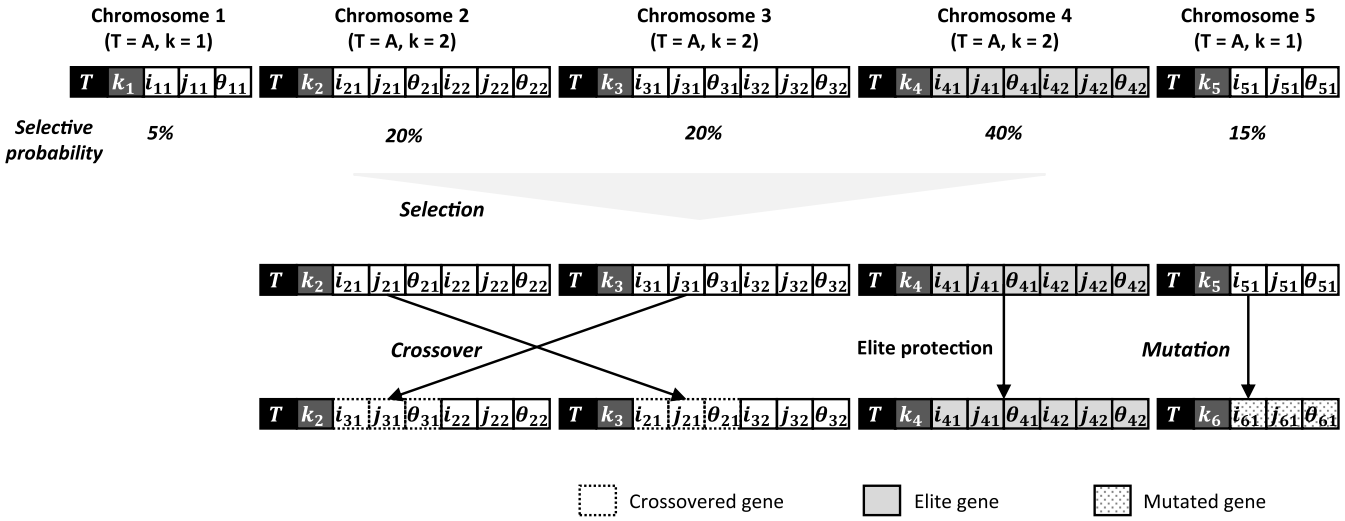

Fig. 5. Concept of sematic-cost genetic algorithm built on proposed framework.

Each chromosome consists of type, number, locations, and orientations of cameras. Camera type T should be primarily fixed because a camera network is assumed to consist of a single type of camera, as described in the problem definition and mathematical modeling. Then, the number of cameras k is determined, and a single chromosome is constructed with additional genes of locations (i, j) and orientation θ for each camera—the total length of a chromosome can be represented as $2 + k \times 3$. Once all of the chromosomes are generated, their selective probabilities according to the fitness values can be calculated and part of the chromosomes based on the assigned probabilities can be selected (e.g., Chromosomes 2, 3, 4, and 5 in this example). Next, Chromosome 4 remains for elite protection and the other chromosomes are fed into the crossover and mutation; the locations and orientations of Chromosomes 2 and 3 are crossovered and all genes in Chromosome 5 are mutated. These evolution processes are repeated until the terminal conditions are satisfied. The defined problem can be additionally constrained based on jobsite-specific conditions. In this paper, two additional constraints [Eqs. (8) and (9)] are considered to be relevant to genes of the number and orientations of cameras. Eq. (8) indicates that the number of cameras is a positive integer value lower than the specific threshold K—which is a reasonably estimated maximum number of cameras to be installed on a given construction jobsite. This constraint enables not testing the highly irrational cases; for instance, a total of 20 cameras are required to cover a small construction site of size 5×5 m. Eq. (9) indicates that the camera orientation is set as a multiple of 5 from 0 to 360 degrees—a total of 73 variables. With the two additional conditions, significantly reducing the search space while maintaining the acceptable level of optimization accuracy in the authors' heuristic experiments is possible. Finally, the total combinations of the search space for a specific camera type can be represented as Eq. (10)

$$1 \leq k \leq K \tag{8}$$

$$mod(\theta, 5) = 0 \tag{9}$$

$$\sum_{k=1}^{K} 73^k \cdot {}_L C_k \cdot k! \tag{10}$$

where the positive integer variable k represents number of cameras to be installed; K represents reasonably estimated maximum number of cameras required to fully cover the entire construction site; θ indicates the camera orientation; and L indicates the total number of installable locations at a given construction site.

Case Study

To evaluate the proposed framework, an actual construction project was examined and three analyses were conducted. First, the total weighted visible coverages were comparatively analyzed between existing camera networks and suggested optimal solutions with the same type and number of cameras. Thereby, the authors aim to confirm the applicability and practicality of the proposed framework in finding optimal camera placement on actual construction jobsites. Second, the research team attempted to find near-global optimums (i.e., Pareto solutions) of camera configurations (i.e., types, number, locations, and orientations) to produce multiple network design alternatives. Finally, based on the Pareto solutions, coverage-cost trade-off analysis was performed to understand the nonlinear relationship between visible coverage and total costs.

Fig. 3(a) illustrates the actual site layout of the construction jobsite where the case study was carried out. The construction project proceeded to extend an existing building and construct two new buildings—presented as "structures" in Fig. 3(a)—at Seoul National University, Seoul, South Korea. The jobsite scale was 70×30 m, and three fixed cameras (visible distance: 32 m, angle of view: 60°) were installed at different streetlights for construction operations/on-site logistics monitoring. The total costs were \$2,100 (\$600 for installation and \$1,500 for purchasing), and the project manager was willing to pay the maximal \$3,000 only if the camera network covers more than the half of the target monitoring areas (including work zones, travel paths, and storage yard). Regarding installable locations, surveillance cameras could be located at every jobsite boundary except the existing building and the two structures that had been being extended given the technical challenges of power accessibility and data transmissibility. The spatial-contextual weights for each target monitoring area were assigned using the bivariate Gaussian distribution.

First, this research compared the performance of the existing camera networks with the suggested solutions. Fig. 6(a) indicates the locations and orientations of the existing cameras and their visible coverage. The total weighted visible coverage rate (WVCR), which means the actual obtained spatial-contextual weights divided by the total obtainable weights [Eq. (11)], was 44.5%. Fig. 6(b) displays the visible coverage of the suggested camera placement and the obtained WVCR was 77.8%. Such a performance gain could be explained based on jobsite-specific conditions. According to the project managers and camera network designers who had placed the cameras on the given jobsite, the cameras were installed at streetlights to minimize installation costs [Fig. 6(c)]—the existing streetlights on jobsites can reduce installation costs related to additional apparatus and labor input. Despite the cost-saving intentions, Camera 2 in the existing network had a large amount of overlapping areas with the other two cameras and yielded few contributions to the performance gain in WVCR [Fig. 6(a)]. Only 1.3% of WVCR was observed to decrease when camera 2 was removed from the existing placement. One interpretation is that the practitioners, including project managers and camera designers, experienced difficulties predicting the occlusion and overlapping effects and estimating the total coverage before installing cameras on actual jobsites. This interpretation is in line with the results of our expert interviews and findings of the previous study (Pålsson and Ståhl 2008)—actual coverage of installed cameras differs from human expectations

$$WVCR = \frac{\sum_{\theta} \sum_{i} \sum_{j} x_{i_1 j_1 \theta_1} e_{i_1 j_1 \theta_1 i_2 j_2} w_{i_2 j_2}}{\sum_{i} \sum_{j} w_{ij}} \tag{11}$$

Second, this study leveraged Pareto solutions to provide project managers with multiple camera placement alternatives. A total of three types of cameras were used, as illustrated in Fig. 1. Visible distances and angle of views for each camera type were computed based on the official AXIS lens calculator (AXIS Communication 2018) and minimal image resolution (32 pixels per meter) for recognizing construction workers (Olshausen et al. 1993). The graph of Fig. 7 illustrates Pareto solutions of each camera type. This coverage-cost graph indicates that, for budgets less than \$2,500, Pareto solutions of camera Type A tends to dominate the other Types B and C, and the lowest WVCR was observed mainly from Type B. This tendency can be further explained using the camera placement simulation results. In Figs. 7(a–c), the authors observed that the coverage shape of camera Type A (long visible distance and small angle of view) is the most geometrically fitted to cover cells with higher spatial-contextual weights—work zones on the given

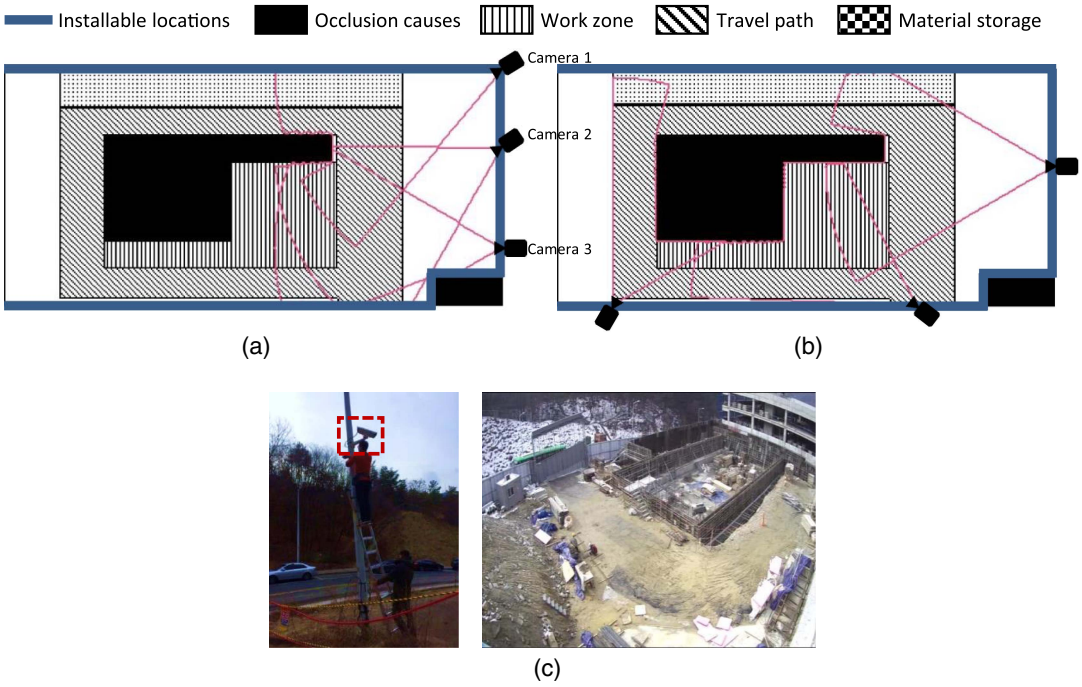

Fig. 6. Visible coverage of installed cameras and jobsite conditions: (a) existing camera network; (b) suggested camera network; and (c) camera installed at streetlight and examples of collected image.

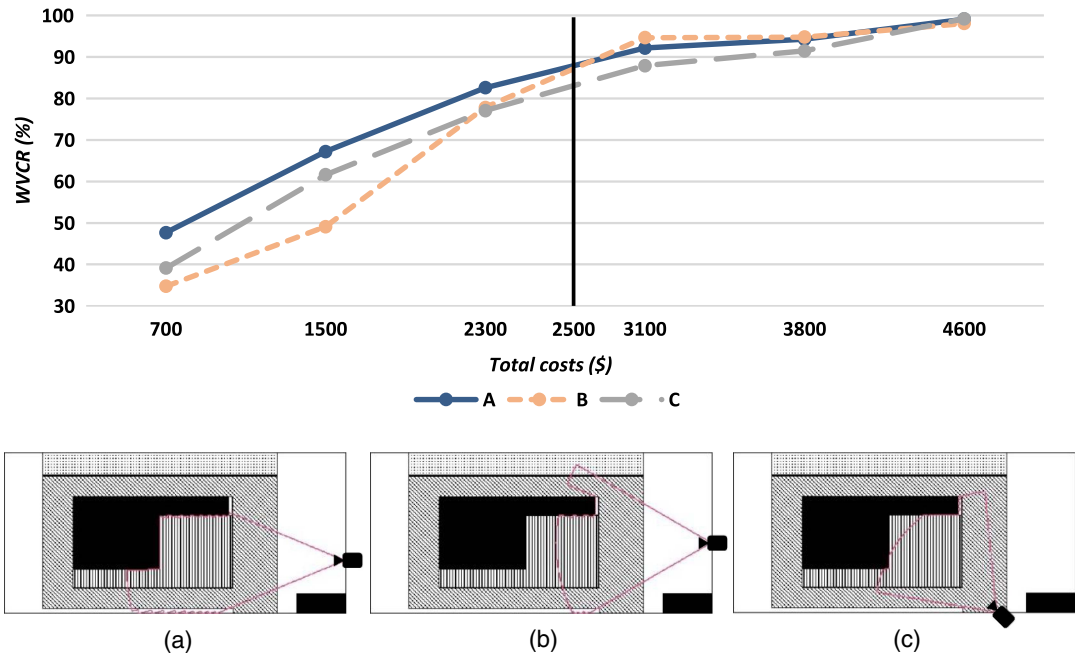

Fig. 7. Graph for Pareto solutions of each camera type and simulation results for single camera of each camera type: (a) Type A; (b) Type B; and (c) Type C.

jobsite. However, such superiority varies with the growth in the budget from \$1,500 to \$3,100 (Fig. 7). At \$2,300, the WVCR of camera Type B becomes greater than that of Type C, and it finally outperforms the other camera types at \$3,100. Based on the simulation results (Fig. 8), that the performance gain (increase in visible coverage) of camera Type B was more noticeable than that of Types A and C with budgets increase from \$1,500 to \$3,100 can be intuitively recognized. In particular, when the budgets increase from \$2,300 to \$3,100, the installation location of an additional camera (fourth camera) to maximize visible coverage gains for camera Type B was obvious but appears complicated for camera Types A and C. The optimization results indicated in Fig. 8 are consistent with our understanding as follows. In the second and third columns of Fig. 8, Type B's camera placements at \$2,300 and

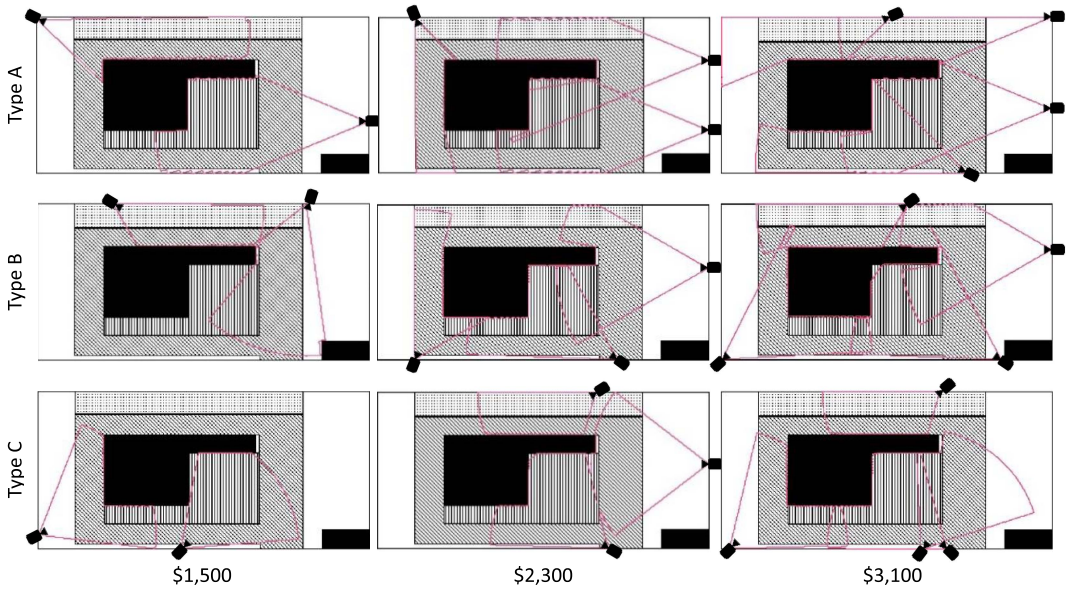

Fig. 8. Example results of suggested camera placement for each camera type and number.

$3,100 are observed to be very similar, indicating that the locations and orientations of the previous three cameras at $2,300 did not change remarkably. In contrast, the camera placements of Types A and C definitely differ between $2,300 and $3,100. The experimental results validate the proposed framework's capability to robustly produce various camera network designs with different number, types, locations, and orientations.

Finally, coverage-cost trade-off analysis was performed to understand the nonlinear relationship between visual monitoring performance (i.e., WVCR) and investment expenses (i.e., total costs). Fig. 9 indicates the maximal and marginal WVCR, and Fig. 10 displays the simulation results of the best solutions suggested by the proposed framework given specified budget constraints. When project managers decide to install a single camera, the recommendation is to locate camera Type A using Solution 1. As can be observed in Fig. 10, Solution 1 can cover most work zones and parts of the travel paths with a total WVCR of 47.7%.

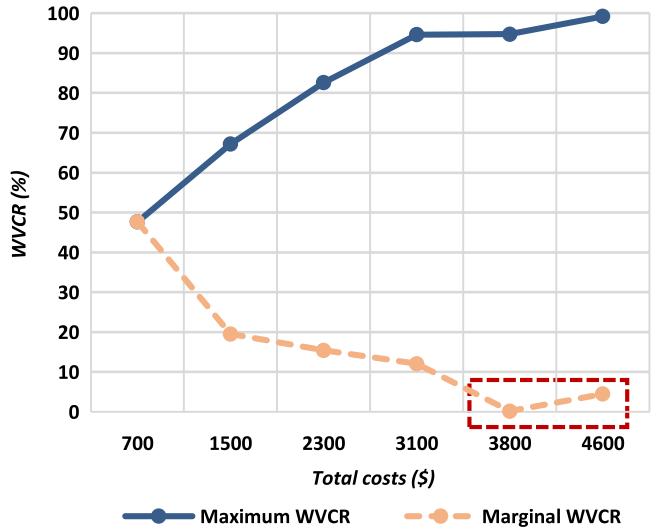

Fig. 9. Coverage-cost trade-off analysis.

If more than 50% of the work zones, travel paths, and storage yards must be monitored with the minimal budgets (as the real project manager mentioned), Solution 2 is preferred. Solution 2 provides not only an adequate WVCR of 67.2% but also the peak marginal WVCR of 19.5% per camera. Solution 3 also has a significant marginal WVCR of 15.4% and even brings a WVCR of more than 80% (Fig. 9). Given its reasonably acceptable performance, the project manager would consider Solution 3 as the best solution, although Solution 2 satisfies all primary constraints: WVCR of more than 50% within budgets of less than $3,000. This improvement tendency continues until the total costs reach $3,100, and WVCR increases up to 94.6% with Solution 4. In contrast, to monitor all of the target areas (approximately 100% WVCR), at least six cameras were observed to be needed and 99.2% WVCR can be obtained using Solution 6. Based on the cost-coverage trade-off analysis, project managers can properly select a solution that satisfies the specific priorities and/or constraints (e.g., budgets, monitoring performance). For instance, project managers would select (1) the lowest total costs that can be achieved within the specified visual monitoring performance (Solution 2) and/or (2) the maximum monitoring performance that complies with constrained budgets (Solution 3). Additionally, only with $100 increases in budgets is Solution 4 a good selection for covering most target monitoring areas with 94.6% WVCR. Through the proposed framework, such a cost-benefit (coverage-cost) trade-off analysis with quantitative information can help project managers make reasonable decisions that are relevant to the camera placement on construction jobsites.

Discussions and Conclusions

For the purpose of operation-level visual monitoring, construction practitioners install surveillance cameras on construction jobsites. However, they often encounter difficulties in planning proper camera placement, and the absence of systematic guidelines makes the challenges more crucial and severe. To address such challenges, this paper proposed a new systematic camera placement framework that incorporates various unique characteristics of construction jobsites. To achieve this, the research team conducted extensive expert interviews to identify the visual monitoring determinants,

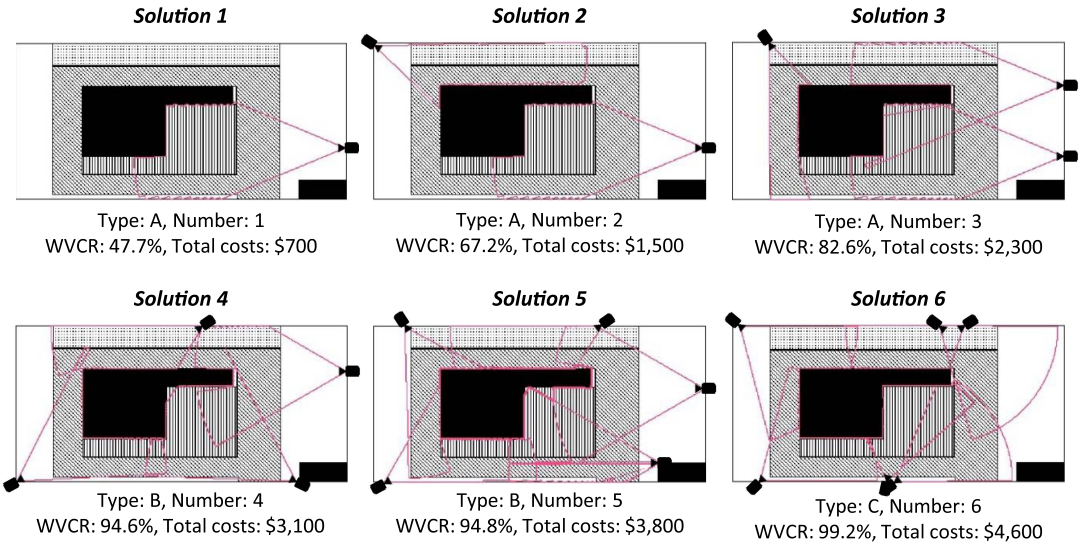

Fig. 10. Results of camera placement simulation of best solutions.

influencing factors, and camera placement conditions to be considered. Next, based on the expert interviews, the authors performed problem definition and mathematical modeling for camera placement optimization. Finally, a new hybrid simulation-optimization process composed of jobsite modeling, camera placement simulation, and semantic-cost genetic algorithm was developed. To validate the proposed framework, a case study was carried out under the jobsite conditions of an actual construction project. The results of the case study showed that the framework has the potential to (1) improve visible coverage for target monitoring areas relative to existing camera networks with the same type and number of cameras; (2) provide construction practitioners with multiple camera network design alternatives by finding Pareto solutions; (3) enhance the understanding of the trade-offs between cameras' visible coverage and total costs; (4) quantify the performance of visual monitoring (WVCR) with the total costs required; and finally (5) support the cost-benefit analysis and decision making for camera placement on complex construction jobsites. In particular, to reflect a wide range of visual monitoring purposes, this study assigned spatial-contextual weights to each cell of the target monitoring areas. The distributed weights assist the semantic-cost GA optimization find camera configurations that cover important spaces with higher spatial-contextual values and provide camera placement specialized for project managers' priorities. Fig. 11 displays the visible coverage of optimized camera placement without the weighting method, which indicates that all of the cells at the jobsite have equal spatial-contextual weights. The results indicate that the surveillance cameras most likely cover a large amount of dead zone, e.g., white areas in Fig. 11, without the weighting methods. As camera experts and visual data analysts pointed out during the interview, the occlusion effects were also incorporated through camera placement simulations. The three main simulation processes (coverage modeling, visibility analysis, and installation cost calculation) could quantify the actual visible coverages and installation costs of suggested camera configurations in the optimization procedures. Given the benefits of the proposed framework, construction practitioners can plan proper camera placement, collect adequate visual data, and perform manual monitoring tasks more effectively. Although several prior studies were carried out on automated visual monitoring systems in construction, visual data collected from actual construction jobsites should have a high enough quality to realize the benefits from computer vision techniques. The proposed framework is believed to provide proper camera network designs that satisfy such underlying assumption by addressing the practical challenges of installing cameras on jobsites (e.g., installable locations) and reducing the negative effects to the data analysis tasks (e.g., unclear field-of-view, heavily occluded views). Thus, this research has the potential to contribute to the automation or semiautomation of operation-level visual monitoring.

Several open research challenges remain to be addressed. For instance, the authors observed that inevitable optimization errors occurred in Solution 5 (five Type B cameras). The marginal WVCR increased at $4,600 (Fig. 9) and the semantic-cost GA optimization might have been stuck at a local optimum for Solution 5. This observation is inconsistent with common sense that the marginal WVCR should decrease as the number of cameras increases because cameras should be primarily installed at the best locations and with orientations that provides the highest marginal WVCR during the optimization procedures. Nonetheless, Solution 5 still provides high performance with 94.7% WVCR, and the negligible errors are easily corrected by project managers based on the visualized camera placement simulation (Fig. 10). Although the observed errors usually occur in general NP-hard optimization

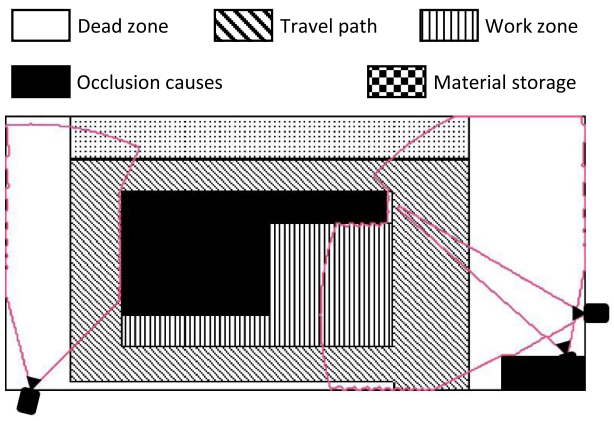

Fig. 11. Examples of optimization results without spatial-contextual weighting.

problems (Ahn et al. 2016), future studies can focus on investigating algorithmic enhancement (e.g., parameter tuning) to avoid being stuck at a local optimum. In contrast, the current semiautomated jobsite modeling involves a manual process by project managers. The spatial modeling process has the potential to be fully automated by extracting site-layout information (e.g., regions of work zones and site facilities) through integration with geographical information systems (GIS) or UAV-based aerial image analysis. In addition to the technical aspects, the proposed framework can be applied to diverse construction projects involving various unique jobsite conditions. Additional various elements in the camera placement framework can be available for identification and incorporation. As a step toward the (semi) automation of operation-level monitoring, the proposed framework can be extended in the future to optimization problems for maximizing the performance of visual data analysis (e.g., construction equipment detection).

Data Availability Statement

Data generated or analyzed during the study are available from the corresponding author by request. Information on the *Journal*'s data-sharing policy can be found here: https://ascelibrary.org/doi/10.1061/(ASCE)CO.1943-7862.0001263.

Acknowledgments

We express a sincere thank you to the interviewees who shared invaluable opinions and recommendations on this research. This material is in part based on work supported by the National Science Foundation (NSF) under CMMI Award #1832187. Any opinions, findings, and conclusions or recommendations expressed in this material are those of the authors and do not necessarily reflect the views of the NSF. This research is also supported by the Basic Science Research Program through the National Research Foundation of Korea (NRF) funded by the Ministry of Science, ICT and Future Planning (2017R1E1A2A01077468).

References

Abdesselam, S., and Z. Baarir. 2018. "Three variants particle swarm optimization technique for optimal cameras network two dimensions placement." *J. Appl. Eng. Sci. Technol.* 4 (1): 37–45.

Abo-Zahhad, M., S. M. Ahmed, N. Sabor, and S. Sasaki. 2014. "A new energy-efficient adaptive clustering protocol based on genetic algorithm for improving the lifetime and the stable period of wireless sensor networks." *Int. J. Energy Inf. Commun.* 5 (3): 47–72.

Ahn, J.-W., T.-W. Chang, S.-H. Lee, and Y. W. Seo. 2016. "Two-phase algorithm for optimal camera placement." *Sci. Program.* 2016: 1–16.

Aissaoui, A., A. Ouafi, P. Pudlo, C. Gillet, Z.-E. Baarir, and A. Taleb-Ahmed. 2017. "Designing a camera placement assistance system for human motion capture based on a guided genetic algorithm." In *Virtual reality*, 1–11. London: Springer.

Albahri, A. H., and A. Hammad. 2017a. "A novel method for calculating camera coverage in buildings using BIM." *J. Inf. Technol. Constr.* 22 (2): 16–33.

Albahri, A. H., and A. Hammad. 2017b. "Simulation-based optimization of surveillance camera types, number, and placement in buildings using BIM." *J. Comput. Civ. Eng.* 31 (6): 04017055. https://doi.org/10.1061/(ASCE)CP.1943-5487.0000704.

Al-Hmouz, R., and S. Challa. 2005. "Optimal placement for opportunistic cameras using genetic algorithm." In *Proc., Int. Conf. on Intelligent Sensors, Sensor Networks and Information Processing*, 337–341. New York: IEEE.

Altahir, A. A., V. S. Asirvadam, N. H. Hamid, P. Sebastian, N. Saad, R. Ibrahim, and S. C. Dass. 2017. "Modeling multicamera coverage for placement optimization." *IEEE Sens. Lett.* 1 (6): 1–4. https://doi.org/10.1109/LSENS.2017.2758371.

Auerbach, C. F., and L. B. Silverstein. 2003. *Qualitative data: An introduction to coding and analysis.* New York: New York University Press.

AXIS Communication. 2017. "AXIS M1125-E network camera." Accessed January 26, 2018. https://www.axis.com/files/datasheet/ds_m1125-e_1603623_en_1702.pdf.

AXIS Communication. 2018. "Lens calculator." Accessed January 26, 2018. https://www.axis.com/global/es/tools/lens-calculator.

Bandyopadhyay, S., and S. K. Pal. 2007. *Classification and learning using genetic algorithms: Applications in bioinformatics and web intelligence*. New York: Springer.

Biggs, S. E., T. D. Banks, J. D. Davey, and J. E. Freeman. 2013. "Safety leaders' perceptions of safety culture in a large Australasian construction organisation." *Saf. Sci.* 52: 3–12. https://doi.org/10.1016/j.ssci.2012.04.012.

Bodor, R., A. Drenner, P. Schrater, and N. Papanikolopoulos. 2007. "Optimal camera placement for automated surveillance tasks." *J. Intell. Rob. Syst.: Theory Appl.* 50 (3): 257–295. https://doi.org/10.1007/s10846-007-9164-7.

Bügler, M., A. Borrmann, G. Ogunmakin, P. A. Vela, and J. Teizer. 2017. "Fusion of photogrammetry and video analysis for productivity assessment of earthwork processes." *Comput.-Aided Civ. Infrastruct. Eng.* 32 (2): 107–123. https://doi.org/10.1111/mice.12235.

Chen, H.-T., S.-W. Wu, and S.-H. Hsieh. 2013. "Visualization of CCTV coverage in public building space using BIM technology." *Visual. Eng.* 1 (1): 5. https://doi.org/10.1186/2213-7459-1-5.

Chi, S., and C. H. Caldas. 2012. "Image-based safety assessment: Automated spatial safety risk identification of earthmoving and surface mining activities." *J. Constr. Eng. Manage.* 138 (3): 341–351. https://doi.org/10.1061/(ASCE)CO.1943-7862.0000438.

Cole, R., and M. Sharir. 1989. "Visibility problems for polyhedral terrains." *J. Symbolic Comput.* 7 (1): 11–30. https://doi.org/10.1016/S0747-7171(89)80003-3.

Ding, L., W. Fang, H. Luo, P. E. D. Love, B. Zhong, and X. Ouyang. 2017. "A deep hybrid learning model to detect unsafe behavior: Integrating convolution neural networks and long short-term memory." *Autom. Constr.* 86: 118–124. https://doi.org/10.1016/j.autcon.2017.11.002.

Fang, Q., H. Li, X. Luo, L. Ding, H. Luo, and C. Li. 2018a. "Computer vision aided inspection on falling prevention measures for steeplejacks in an aerial environment." *Autom. Constr.* 93: 148–164. https://doi.org/10.1016/j.autcon.2018.05.022.

Fang, Q., H. Li, X. Luo, L. Ding, H. Luo, T. M. Rose, and W. An. 2018b. "Detecting non-hardhat-use by a deep learning method from far-field surveillance videos." *Autom. Constr.* 85: 1–9. https://doi.org/10.1016/j.autcon.2017.09.018.

Fang, W., L. Ding, H. Luo, and P. E. D. Love. 2018c. "Falls from heights: A computer vision-based approach for safety harness detection." *Autom. Constr.* 91: 53–61. https://doi.org/10.1016/j.autcon.2018.02.018.

Foster, P. L. 2000. "Adaptive mutation: Implications for evolution." *BioEssays: News Rev. Mol. Cell. Dev. Biol.* 22 (12): 1067–1074. https://doi.org/10.1002/1521-1878(200012)22:12%3C1067::AID-BIES4%3E3.0.CO;2-Q.

Golparvar-Fard, M., A. Heydarian, and J. C. Niebles. 2013. "Vision-based action recognition of earthmoving equipment using spatio-temporal features and support vector machine classifiers." *Adv. Eng. Inf.* 27 (4): 652–663. https://doi.org/10.1016/j.aei.2013.09.001.

Gonzalez-Barbosa, J.-J., T. Garcia-Ramirez, J. Salas, J.-B. Hurtado-Ramos, and J.-D.-J. Rico-Jimenez. 2009. "Optimal camera placement for total coverage." In *Proc., IEEE Int. Conf. on Robotics and Automation*, 844–848. New York: IEEE.

Ham, Y., K. K. Han, J. J. Lin, and M. Golparvar-Fard. 2016. "Visual monitoring of civil infrastructure systems via camera-equipped Unmanned Aerial Vehicles (UAVs): A review of related works." *Visual. Eng.* 4 (1): 1. https://doi.org/10.1186/s40327-015-0029-z.

Han, S., and S. Lee. 2013. "A vision-based motion capture and recognition framework for behavior-based safety management." *Autom. Constr.* 35: 131–141. https://doi.org/10.1016/j.autcon.2013.05.001.

Hörster, E., and R. Lienhart. 2006. "On the optimal placement of multiple visual sensors." In *Proc., 4th ACM Int. Workshop on Video Surveillance and Sensor Networks (VSSN'06)*, 111. New York: ACM Press.

Indu, S., S. Chaudhury, N. R. Mittal, and A. Bhattacharyya. 2009. "Optimal sensor placement for surveillance of large spaces." In *Proc., 3rd ACM/IEEE Int. Conf. on Distributed Smart Cameras (ICDSC)*, 1–8. New York: IEEE.

Kim, H., S. Bang, H. Jeong, Y. Ham, and H. Kim. 2018a. "Analyzing context and productivity of tunnel earthmoving processes using imaging and simulation." *Autom. Constr.* 92: 188–198. https://doi.org/10.1016/j.autcon.2018.04.002.

Kim, H., K. Kim, and H. Kim. 2016. "Vision-based object-centric safety assessment using fuzzy inference: Monitoring struck-by accidents with moving objects." *J. Comput. Civ. Eng.* 30 (4): 04015075. https://doi.org/10.1061/(ASCE)CP.1943-5487.0000562.

Kim, J., and S. Chi. 2017. "Adaptive detector and tracker on construction sites using functional integration and online learning." *J. Comput. Civ. Eng.* 31 (5): 04017026. https://doi.org/10.1061/(ASCE)CP.1943-5487.0000677.

Kim, J., S. Chi, and J. Seo. 2018d. "Interaction analysis for vision-based activity identification of earthmoving excavators and dump trucks." *Autom. Constr.* 87: 297–308. https://doi.org/10.1016/j.autcon.2017.12.016.

Luo, H., C. Xiong, W. Fang, P. E. D. Love, B. Zhang, and X. Ouyang. 2018b. "Convolutional neural networks: Computer vision-based workforce activity assessment in construction." *Autom. Constr.* 94: 282–289. https://doi.org/10.1016/j.autcon.2018.06.007.

Luo, X., H. Li, D. Cao, F. Dai, J. Seo, and S. Lee. 2018c. "Recognizing diverse construction activities in site images via relevance networks of construction-related objects detected by convolutional neural networks." *J. Comput. Civ. Eng.* 32 (3): 04018012 https://doi.org/10.1061/(ASCE)CP.1943-5487.0000756.

Luo, X., H. Li, D. Cao, Y. Yu, X. Yang, and T. Huang. 2018d. "Towards efficient and objective work sampling: Recognizing workers' activities in site surveillance videos with two-stream convolutional networks." *Autom. Constr.* 94: 360–370. https://doi.org/10.1016/j.autcon.2018.07.011.

Morsly, Y., N. Aouf, and M. Djouadi. 2009. "On the optimal placement of multiple visual sensor based binary particle swarm optimization." *IFAC Proc. Vol.* 42 (19): 279–285. https://doi.org/10.3182/20090921-3-TR-3005.00050.

Murray, A. T., K. Kim, J. W. Davis, R. Machiraju, and R. Parent. 2007. "Coverage optimization to support security monitoring." *Comput. Environ. Urban Syst.* 31 (2): 133–147. https://doi.org/10.1016/j.compenvurbsys.2006.06.002.

Nguyen, H. T., and B. Bhanu. 2011. "VideoWeb: Optimizing a wireless camera network for real-time surveillance." In *Distributed video sensor networks*, 321–334. London: Springer.

Olague, G., and R. Mohr. 2002. "Optimal camera placement for accurate reconstruction." *Pattern Recognit.* 35: 927–944. https://doi.org/10.1016/S0031-3203(01)00076-0.

Olshausen, B. A., C. H. Anderson, and D. C. Van Essen. 1993. "A neurobiological model of visual attention and invariant pattern recognition based on dynamic routing of information." *J. Neurosci.: Off. J. Soc. Neurosci.* 13 (11): 4700–4719. https://doi.org/10.1523/JNEUROSCI.13-11-04700.1993.

O'Rourke, J. 1987. *Art gallery theorems and algorithms.* New York: Oxford University Press.

Pålsson, M., and J. Ståhl. 2008. "The camera placement problem: An art gallery problem variation." Master thesis, Dept. of Computer Science, Lund Univ.

Park, M.-W., N. Elsafty, and Z. Zhu. 2015. "Hardhat-wearing detection for enhancing on-site safety of construction workers." *J. Constr. Eng. Manage.* 141 (9): 04015024. https://doi.org/10.1061/(ASCE)CO.1943-7862.0000974.

Rahimian, P., and J. K. Kearney. 2017. "Optimal camera placement for motion capture systems." *IEEE Trans. Visual Comput. Graphics* 23 (3): 1209–1221. https://doi.org/10.1109/TVCG.2016.2637334.

Rezazadeh Azar, E., S. Dickinson, and B. McCabe. 2013. "Server-customer interaction tracker: Computer vision–based system to estimate dirt-loading cycles." *J. Constr. Eng. Manage.* 139 (7): 785–794. https://doi.org/10.1061/(ASCE)CO.1943-7862.0000652.

Seo, J., S. Han, S. Lee, and H. Kim. 2015. "Computer vision techniques for construction safety and health monitoring." *Adv. Eng. Inf.* 29 (2): 239–251. https://doi.org/10.1016/j.aei.2015.02.001.

Spall, J. C. 2003. *Introduction to stochastic search and optimization: Estimation, simulation, and control.* Hoboken, NJ: Wiley-Interscience.

Szaloki, D., N. Koszo, K. Csorba, and G. Tevesz. 2013. "Optimizing camera placement for localization accuracy." In *Proc., 14th IEEE Int. Symp. on Computational Intelligence and Informatics (CINTI 2013)*, 207–212. New York: IEEE.

Teizer, J. 2015. "Status quo and open challenges in vision-based sensing and tracking of temporary resources on infrastructure construction sites." *Adv. Eng. Inf.* 29 (2): 225–238. https://doi.org/10.1016/j.aei.2015.03.006.

Yang, J., M.-W. Park, P. A. Vela, and M. Golparvar-Fard. 2015. "Construction performance monitoring via still images, time-lapse photos, and video streams: Now, tomorrow, and the future." *Adv. Eng. Inf.* 29 (2): 211–224. https://doi.org/10.1016/j.aei.2015.01.011.

Zhang, H., S. Chi, J. Yang, M. Nepal, and S. Moon. 2017. "Development of a safety inspection framework on construction sites using mobile computing." *J. Manage. Eng.* 33 (3): 04016048. https://doi.org/10.1061/(ASCE)ME.1943-5479.0000495.

Zhao, J., R. Yoshida, S. S. Cheung, and D. Haws. 2013. "Approximate techniques in solving optimal camera placement problems." *Int. J. Distrib. Sens. Netw.* 9 (11): 241913. https://doi.org/10.1155/2013/241913.